

Published in final edited form as:

*Sci Signal*. ; 7(330): ra57. doi:10.1126/scisignal.2004838.

## A FAK-Cas-Rac-Lamellipodin Signaling Module Transduces Extracellular Matrix Stiffness into Mechanosensitive Cell Cycling

Yong Ho Bae<sup>1,\*</sup>, Keeley L. Mui<sup>1</sup>, Bernadette Y. Hsu<sup>1</sup>, Shu-Lin Liu<sup>1</sup>, Alexandra Cretu<sup>1</sup>, Ziba Razinia<sup>1</sup>, Tina Xu<sup>1</sup>, Ellen Puré<sup>2</sup>, and Richard K. Assoian<sup>1,\*</sup>

<sup>1</sup>Department of Pharmacology, Perelman School of Medicine, University of Pennsylvania, Philadelphia, PA 19104

<sup>2</sup>Department of Animal Biology, School of Veterinary Medicine, University of Pennsylvania, Philadelphia, PA 19104

### Abstract

Tissue and extracellular matrix (ECM) stiffness is transduced into intracellular stiffness, signaling, and changes in cellular behavior. Integrins and several of their associated focal adhesion proteins have been implicated in sensing ECM stiffness. We investigated how an initial sensing event is translated into intracellular stiffness and a biologically interpretable signal. We found that a pathway consisting of focal adhesion kinase (FAK), the adaptor protein p130Cas (Cas), and the guanosine triphosphatase Rac selectively transduced ECM stiffness into stable intracellular stiffness, increased abundance of the cell cycle protein cyclin D1, and promoted S phase entry. Rac-dependent intracellular stiffening involved its binding partner lamellipodin, a protein that transmits Rac signals to the cytoskeleton during cell migration. Our findings establish that mechanotransduction by a FAK-Cas-Rac-lamellipodin signaling module converts the external information encoded by ECM stiffness into stable intracellular stiffness and mechanosensitive cell cycling. Thus, lamellipodin is not only important in controlling cellular migration, but also for regulating the cell cycle in response to mechanical signals.

### INTRODUCTION

Mechanical forces play a critical role in regulating cellular function (1–6). In vivo, cells are exposed to mechanical forces as a consequence of blood flow, interstitial flow, blood pressure, and extracellular matrix (ECM) stiffness. Pathological microenvironments, such as those seen in tumors, cardiovascular disease, and lung and liver fibrosis, are often stiffer than their physiological counterparts. Indeed, mechanical signals arising from a stiff ECM

\*To whom correspondence should be addressed. yob@mail.med.upenn.edu or assoian@mail.med.upenn.edu.

**AUTHOR CONTRIBUTIONS:** Project and experimental designs were performed by Y.H.B., K.L.M., Z.R., and R.K.A. Experiments were performed by Y.H.B., K.L.M., B.Y.H., S-L.L., A.C., Z.R., and T.X. Data analyses were performed by Y.H.B., K.L.M., B.Y.H., S.L.L., A.C., Z.R., T.X., and R.K.A. The bioinformatic analysis was performed by R.K.A. Statistical tests were performed by Y.H.B. and R.K.A. Y.H.B., K.L.M., B.Y.H., E.P., and R.K.A. wrote and edited the manuscript.

**MATERIALS AND DATA AVAILABILITY:** The floxed Rac1 mouse requires a materials transfer agreement (MTA) from National Institute of Medical Research. The inducible Cre mouse requires an MTA from the Max Planck Institute for Heart and Lung Research. The gene expression data has been deposited in Gene Expression Omnibus (dataset GSE40637).

**COMPETING INTERESTS:** The authors declare that they have no competing interests.

contribute to pathological cellular responses such as increased migration and aberrant proliferation (6–9). Conversely, tissue softening inhibits tumor formation and atherosclerosis (5, 7–9).

The information encoded by tissue and ECM stiffness is transduced into intracellular stiffness and force by integrins, the transmembrane adhesion receptors for ECM proteins, their associated focal adhesion proteins, and the actin cytoskeleton (10–14). Several focal adhesion proteins, including focal adhesion kinase (FAK), the adapter proteins p130Cas (Cas) and paxillin, and the cytoskeletal protein vinculin have been implicated in the initial stiffness-sensing event (13, 15–22). However, the mechanism by which ECM stiffness is transduced into intracellular stiffness and stiffness-dependent cell cycling, and whether these processes are mediated by all or some of the stiffness-sensing focal adhesion proteins, remains largely unknown.

To understand the role of tissue and ECM stiffness in regulating intracellular stiffness, signaling, and cellular function, it is essential to study signaling under conditions that recapitulate the range of physiological stiffness found in vivo. Stiffness-dependent signaling cannot be analyzed with traditional cell culture on nondeformable (rigid) substrata that do not model the elasticity of pathophysiologic microenvironments. Here we have used deformable substrata of biologically relevant elastic moduli, bioinformatics and mouse models to elucidate a mechanosensitive signaling pathway that propagates an initial stiffness-sensing event into stable intracellular stiffness and cell cycling.

## RESULTS

### Stiffness-mediated FAK signaling to Cas selectively transduces ECM stiffness into mechanosensitive cell cycling

Previous studies have shown that mitogen-stimulated cell cycling is blocked when mouse embryo fibroblasts (MEFs), vascular smooth muscle cells (VSMCs), or mammary epithelial cells are cultured on low stiffness substrata (2–4 KPa) whereas high stiffness substrata (20–25 KPa) permit cell cycling (13). To identify focal adhesion proteins that transduce ECM stiffness into cell cycling, we examined the phosphorylation states of different focal adhesion proteins in serum-stimulated MEFs on fibronectin-coated, low and high stiffness hydrogels. The high stiffness substratum stimulated phosphorylation of Cas at Tyr<sup>410</sup>, one of 15 tyrosine residues in the substrate binding domain that serves as a docking site for proteins with SH2 domains including Crk, Nck, and SHIP2 (23–25) (Fig. 1A). Phosphorylation of paxillin at Tyr<sup>118</sup> (a major tyrosine phosphorylation site that enables binding to Crk (26, 27)) (Fig. 1B) and of vinculin at Tyr<sup>822</sup> (a residue involved in focal adhesion integrity and apoptosis (28)) (Fig. 1C) were also sensitive to the stiffness of the substratum. In addition to MEFs, stiffness-sensitive phosphorylation of FAK, Cas, and paxillin occurred in primary mouse VSMCs (Fig. S1A).

We then determined the ability of these stiffness-sensing focal adhesion proteins to affect cell cycling. siRNA was used to acutely knock-down Cas, paxillin and vinculin (Fig. S1B–C). Knock-down of Cas, but not paxillin or vinculin, reduced S phase entry as shown by EdU incorporation (Fig. 1D) and the induction of cyclin A (an E2F target gene and S phase

marker) (Fig. S1B–C) when MEFs were cultured on the high stiffness substratum. The percentage of Cas knock-down cells in S phase was similar to that of control MEFs plated on the low stiffness substratum (Fig. 1D), and this decrease in the percentage of cells in S phase occurred without apparent disruption of overall focal adhesion structure because paxillin and vinculin staining retained their characteristic focal adhesion staining pattern when Cas-null cells were cultured on the high stiffness substratum (Fig. S1D). Thus, Cas selectively transduces ECM stiffness into cell cycling.

Cas can be phosphorylated by FAK and Src (24, 25, 29–31), and several lines of evidence indicated that FAK, Src, and Cas comprise a signaling module that transduces ECM stiffness into intracellular stiffness and cell cycling. We first established a role for FAK by demonstrating that FAK phosphorylation at its autophosphorylation site (Tyr<sup>397</sup>) and two sites targeted by Src (Tyr<sup>576</sup> and Tyr<sup>861</sup>) were sensitive to the stiffness of the substratum (Fig. 1E) and that FAK inhibition with FRNK (FAK-related nonkinase) or FAK<sup>397F</sup> (a non-phosphorylatable form of FAK) reduced the stiffness-sensitivity of Cas phosphorylation at Tyr<sup>410</sup> (Fig. 1F). We then demonstrated a role for Src by showing that the phosphorylation of Cas at Tyr<sup>410</sup> seen on the high stiffness substratum was reduced in MEFs lacking Src-family kinases (SYF-null) and restored upon reconstitution of SYF cells with c-Src (Fig. 1G). However, unlike FAK and Cas, the extent of phosphorylation of regulatory sites in Src was similar in serum-stimulated cells cultured on low or high stiffness substrata (Fig. S1E). The stiffness-sensitive phosphorylation of FAK and Cas and the stiffness-insensitive phosphorylation of Src were readily detected from 1 through 20 hours of mitogenic stimulation (Fig. S1E).

Src forms a complex with autophosphorylated FAK, enabling phosphorylation of FAK at Src sites (31, 32). Consistent with this model, the degree of FAK phosphorylation at two Src sites (Tyr<sup>576</sup> and Tyr<sup>861</sup>) was similar to that of stiffness-sensitive FAK autophosphorylation (Fig. 1E). These results suggested that the degree of FAK/Src complex formation is set by the stiffness sensitivity of autophosphorylation of FAK.

### A FAK-Cas-Rac signaling module transduces ECM stiffness into intracellular stiffness

We used atomic force microscopy (AFM) to examine the role of FAK and Cas in mediating intracellular stiffness. When plated on high ECM stiffness hydrogels, FAK inhibition with FRNK or deletion of Cas in MEFs reduced intracellular stiffness (Fig. 2A; columns 3–4) as compared to wild-type MEFs (Fig. 2A; column 2). Thus, FAK and Cas are required to transduce extracellular stiffness into intracellular stiffness. Moreover, intracellular stiffness was restored when Cas-null MEFs were reconstituted with full-length Cas (Fig. 2A; column

---

#### SUPPLEMENTARY MATERIALS

- Fig. S1. Stiffness-dependent regulation of focal adhesion proteins and cell cycling.  
 Fig. S2. Effect of time and stiffness-dependent Rac activity on intracellular stiffness.  
 Fig. S3. Regulation of Rac activity by CrkII.  
 Fig. S4. A FAK-Cas signaling module is necessary for cyclin D1 induction in MEFs and VSMCs.  
 Fig. S5. Bioinformatic identification of a FAK/Rac signaling pathway to cyclin D1  
 Fig. S6. Morphology of uninjured femoral arteries from Rac1<sup>fl/fl</sup>;SM-iCre mice.  
 Fig. S7. Effect of lamellipodin knockdown on FAK and Cas phosphorylation and cyclin D1 induction.  
 Fig. S8. Dose-dependent inhibition of FAK autophosphorylation and Rac-GTP loading by PF573228 and NSC23766.  
 Table S1. Cell cycle genes that are differentially expressed after vascular injury

5) but not when they were reconstituted with Cas mutants lacking the CrkII- (Cas<sup>15F</sup>) or FAK- (Cas<sup>SH3</sup>) binding domains (Fig. 2A; columns 6–7). These results link the effects of FAK-Cas signaling on mechanosensitive cell cycling to intracellular stiffening.

Intracellular stiffness is largely regulated by actin polymerization and remodeling which are, in turn, controlled by the Rho family GTPases: Rho, Rac and Cdc42 (33–38). We previously reported that FAK activity is required for Rac activation on high stiffness hydrogels and that constitutively active Rac rescues expression of cyclin D1 mRNA on low stiffness hydrogels (13). Because Rac is a major target of Cas (39–41), we examined the role of Cas in stiffness-mediated Rac activation and intracellular stiffening. The activation of Rac persisted for up to 9 hours after serum stimulation of cells on high-stiffness hydrogels (Fig. S2A), and siRNAs directed against Cas reduced Rac-GTP loading (Fig. 2B). Moreover, the inhibitory effect of Cas knockout on intracellular stiffness (Fig. 2A) was phenocopied by expressing dominant negative Rac (Rac<sup>N17</sup>; Fig. 2C) or treating cells with the pharmacological Rac inhibitor NSC23766 (Fig. S2B). Conversely, expression of activated Rac (Rac<sup>V12</sup>) rescued intracellular stiffening (Fig. 2D) and cell cycling as measured by cyclin A abundance (Fig. 2E) in MEFs plated on low stiffness hydrogels.

Cas stimulates Rac activity through its interaction with the adapter protein CrkII and the Rac GEF DOCK180 (24, 25, 39–41), and our analysis with Cas mutants (Fig. 2A) indicated that a Cas-CrkII pathway stimulated intracellular stiffening. Consistent with this result, siRNA-mediated knock-down of CrkII inhibited Rac activity in cells on the high stiffness hydrogels (Fig. S3A). Like Src (Fig. S1E), the abundance and phosphorylation of CrkII or DOCK180 (the intermediary protein between CrkII and Rac) were similar in cells on soft and stiff hydrogels (Fig. S3B). We conclude that activation of FAK, Cas, and Rac are the mechanosensitive events within a FAK/Src-Cas-CrkII-DOCK180-Rac signaling pathway that transduces extracellular into intracellular stiffness and mechanosensitive cell cycling.

### **Sustained intracellular stiffening by Rac is required for the mechanosensitive induction of cyclin D1**

The activation of Rac is generally required for the induction of cyclin D1 (13, 42–44). We therefore asked if the upstream regulators of Rac activity described above controlled the stiffness-sensitive abundance of cyclin D1. siRNAs directed against Cas or Crk, expression of interfering mutants for FAK, or deficiency in Src family kinases, reduced the abundance of cyclin D1 protein (Fig. 3A–C). Knock-down of Cas or inhibition of FAK reduced the abundance of not only cyclin D1 protein, but also cyclin D1 mRNA (Fig. S4A). Additionally, cyclin D1 abundance was reduced in primary VSMCs treated with Cas siRNA or Ad-FAK<sup>397F</sup> (Fig. S4B). In contrast, knock-down of paxillin did not affect the protein or mRNA abundance of cyclin D1 in either MEFs or VSMCs (Fig. 3A, S4A–B).

Cas-null MEFs on high stiffness substrata showed reduced S phase entry (Fig. 3D; Ad-LacZ), an effect that was rescued by ectopic expression of cyclin D1 (Fig. 3D; Ad-Cyclin D1). Conversely, cyclin D1 abundance was restored in Cas-null MEFs cultured on stiff substrata upon reconstitution with full-length Cas but not with Cas mutants lacking the CrkII- (Cas<sup>15F</sup>) or FAK- (Cas<sup>SH3</sup>) binding domains (Fig. 3E). An activated Rac allele (Rac<sup>V12</sup>) also restored cyclin D1 abundance in cells on low stiffness substrata (Fig. 3F;

DMSO). These effects on cyclin D1 were not secondary to cycling because the experiments we performed measured changes in cyclin D1 that occurred before S phase. Thus, stiffness-sensitive signaling through the FAK-Cas-Rac module explains stiffness-sensitive cyclin D1 induction and cell cycling.

### **Rac-dependent intracellular stiffening feeds back to maintain signaling through FAK and Cas**

Actin depolymerization with latrunculin B prevented the induction of cyclin D1 (Fig. 3F; LatB) and intracellular stiffening (Fig. 4A), even in cells expressing a constitutively activated Rac (Rac<sup>V12</sup>). This result suggested that actin-dependent cytoskeletal remodeling is required for both intracellular stiffening and the increase in cyclin D1 abundance. To determine how these two events are causally related, we inhibited endogenous Rac activity with Rac<sup>N17</sup> and then treated these cells with jasplakinolide, an actin binding macrocyclic peptide that enhances the rate of actin polymerization and stabilizes actin filaments (45). Jasplakinolide increased intracellular stiffness in Rac-inhibited cells (Fig. 4B) but did not rescue cyclin D1 abundance when Rac was either knocked down or inhibited (Fig. 4C). We conclude that actin-dependent intracellular stiffening is necessary but not sufficient for the induction of cyclin D1; direct Rac signaling to cyclin D1 plays a complementary essential role.

Because cell proliferation occurs over many hours, we reasoned that stable intracellular stiffening would be required for cell cycling if FAK and Rac activities were needed beyond their initial stiffness-induced activation. To determine the kinetic requirements for FAK and Rac, we treated MEFs with pharmacological inhibitors of FAK (PF573228) and Rac (NSC23766) at selected times after mitogenic stimulation. Induction of cyclin D1 and cyclin A (as markers for cell cycling) required persistent activity (> 3 hours) of FAK (Fig. 4E and F) and Rac (Fig. 4G and H). These results suggested that Rac-dependent intracellular stiffening feeds back to maintain the FAK-Cas-Rac signaling module in an activated state (Fig. 4I).

To test this feed-back model directly, we added NSC23766 to MEFs on high stiffness hydrogels that had been pre-incubated with 10% FBS and asked if Rac inhibition could reverse pre-existing FAK and Cas phosphorylation. Indeed, we found that NSC23766 blocked FAK and Cas phosphorylation (Fig. 4J) when it was added 1 or even 3 hours after mitogenic stimulation. Thus, Rac activity is required for the stable activation of FAK and Cas.

### **Rac1 is essential for the proliferative response to vascular injury in vivo**

We used the response to vascular injury as a model to test the effect of mechanosensitive signaling pathways in vivo. In this model, a thin wire is inserted into the lumen of the mouse femoral artery and removed, thereby damaging the endothelial lining of the vessel and leading to local platelet aggregation and release of platelet mitogens including platelet-derived growth factor (PDGF). VSMCs that comprise the underlying arterial medial layer respond to the injury by dedifferentiating, migrating, and proliferating, ultimately forming a smooth muscle-rich "neointima." These dedifferentiated VSMCs produce relatively large

amounts of ECM which remodel the local matrix (46, 47) and stiffen the VSMC microenvironment from 2–4 to 10–20 kPa (13). Stiffened sites of vascular injury contain relatively large numbers of cycling VSMCs as compared to uninjured controls (13) as well as increased amounts of cyclin D1 (Fig. 5A).

We used vascular injury to examine the global expression of genes that are differentially expressed during VSMC proliferation in vivo and dependent on the mechanical signaling pathway described here. The list of genes differentially expressed after vascular injury was compared to the 2019 genes in the "Cell Cycle" functional grouping of Ingenuity Pathway Analysis, and 281 genes were common to both gene lists (Table S1). We then used Path Explorer to identify genes that were downstream of FAK (PTK2) and Rac1. This analysis identified only 5 genes, and cyclin D1 (CCND1) was the only member of the cyclin-cdk network in that data set (Fig. S5). These results further suggest coupling of FAK-Rac signaling to cyclin D1 in vivo.

We next assessed the response to vascular injury in mice harboring a floxed Rac1 allele and a smooth muscle cell-specific, tamoxifen-inducible Cre. The mice were treated with vehicle or tamoxifen at ~4 months to circumvent potential roles for Rac1 in development. Uninjured arteries of vehicle- and tamoxifen-treated mice were grossly indistinguishable (Fig. S6). However, excision of *Rac1* with tamoxifen strongly reduced neointimal formation and cell proliferation as measured by luminal stenosis (percent occluded lumen) (Fig. 5B–C) and EdU labeling (Fig. 5D–E), respectively. Additionally, the abundance of cyclin D1 was low in the medial (M) and neointimal (NI) layers of injured arteries lacking Rac1 (Fig. 5F). Consistent with the mechanosensitive feedback loop identified above, phosphorylation of Cas was reduced in the VSMCs of Rac-null arteries after injury (Fig. 5G).

### **Rac-dependent intracellular stiffening and cyclin D1 induction depend on lamellipodin**

We used AFM in force-volume-mode to generate stiffness and height maps of cells cultured on fibronectin-coated low and high stiffness hydrogels and assess the spatial relationship between ECM stiffness and intracellular stiffening. We found that the intracellular stiffening was most pronounced at the cell periphery (Fig. 6A).

Lamellipodin is thought to promote peripheral actin remodeling as a consequence of its binding to Ena/VASP proteins, actin-binding proteins that localize to focal adhesions at the leading edge of lamellipodia and antagonize actin filament capping (48–50). Moreover, active Rac stimulates a direct interaction between lamellipodin and the Scar/WAVE complex (51). This complex interacts with Arp2/3 to regulate actin filament branching (52, 53). Thus, lamellipodin is poised to regulate actin cytoskeletal dynamics. Indeed we found that the amount of peripheral lamellipodin increased in response to active Rac (Fig. 6B), and this increase reflected translocation as it occurred without a change in total lamellipodin abundance (Fig. 6C). Moreover, knock-down of lamellipodin with a pool of siRNAs reduced peripheral intracellular stiffening (Fig. 6D), the phosphorylation of Tyr<sup>397</sup> in FAK and Tyr<sup>410</sup> in Cas, and the total abundance of cyclin D1 in cells cultured on stiff hydrogels (Fig. 6E). Two individual lamellipodin siRNAs had similar inhibitory effects on FAK and Cas phosphorylation as well as cyclin D1 abundance (Fig. S7). Thus, Rac-dependent

translocation of lamellipodin contributes to peripheral intracellular stiffening and stiffness-sensitive cell cycling.

## DISCUSSION

We show here that a FAK-Cas-Rac signaling module selectively transduces ECM stiffness into intracellular stiffness and mechanosensitive cell cycling. Our work also reveals a tripartite role for Rac as the downstream target of FAK-Cas signaling, the regulator of actin-dependent stiffening that maintains the FAK-Cas-Rac module in an activated state, and a necessary signaling component in the induction of cyclin D1 (Fig. 4I). The importance of this multi-pronged effect is demonstrated by our finding that neither Rac activity alone nor intracellular stiffness alone supports mechanosensitive cell cycling. The distinguishing feature of stiffness-sensitive FAK-Cas-Rac signaling is its ability to create a positive feedback loop that perpetuates mechanosensitive FAK-Cas-Rac activity, intracellular stiffness, and stiffness-dependent cycling (Fig. 4I).

Integrins and several of its associated focal adhesion proteins have been implicated as mechanotransducers that sense ECM stiffness and lead to stiffness-sensitive proliferation. Sawada *et al.* have demonstrated that stretch-mediated force extends Cas to open the substrate binding domain and permit Src-mediated phosphorylation (17). Chen *et al.* have shown that activation of FAK in focal adhesions is induced by cellular stretching (54). We and others have shown that FAK activation is required for stiffness-sensitive cyclin D1 expression (6, 8, 13). However, these studies do not address the mechanism by which ECM stiffness is transduced into stable intracellular stiffness, nor how intracellular stiffness and mechano-signaling cooperate to regulate cellular responses. Our data revealed that only a subset of the documented mechanosensors (FAK and Cas but not vinculin or paxillin) control both intracellular stiffness and stiffness-dependent cycling. Moreover, integrin-mediated adhesion and the activity of FAK and Src stimulate the phosphorylation of paxillin and vinculin as well as that of Cas (22, 24–26, 31), yet we found that only Cas regulated stiffness-dependent cell cycling. These results indicate that FAK signaling to Cas is the critical mechanosensory event in the proliferative response to a stiff ECM.

Rho activity is also stiffness-sensitive (7, 13), and Rho and FAK activities are interdependent (7, 55). Yet expression of activated Rho, as opposed to activated Rac, failed to overcome the stiffness requirement for cell cycling as assessed by the induction of cyclin D1 (13). These results suggest that cortical actin, rather than actin stress fibers, play the critical role in transducing intracellular stiffness into cell cycling, a notion supported by our studies of lamellipodin, a potent regulator of cortical actin polymerization.

We found that Rac activity promotes lamellipodin localization to the cell periphery. Moreover, siRNA-mediated knock-down of lamellipodin reduces both intracellular stiffening and stiffness-dependent cyclin D1 induction. SRF (serum response factor), MRTF (myocardin-related transcription factor) and YAP and TAZ have been implicated in mechanosensitive gene expression (56–59). MRTF is sequestered in the cytoplasm by G-actin and released for translocation into the nucleus where it cooperates in the induction of SRF-dependent transcription. Lamellipodin depletion inhibits SRF activity (60), and the

present study raises the possibility that stimulation of SRF activity by lamellipodin could be a consequence of its effect on actin-mediated intracellular stiffening. Likewise, cytoplasmic sequestration and activity of the transcriptional co-activators, YAP and TAZ, are regulated by ECM stiffness and actin remodeling; these effects contribute to cell growth and proliferation (61, 62). Requirements for MRTF/SRF and/or YAP/TAZ in mechanosensitive cell proliferation may explain why we find that actin-dependent intracellular stiffening is needed for cyclin D1 induction even when cells on low stiffness substrata express activated Rac.

The proliferative response to vascular injury enables an assessment of the biological importance of mechanosensitive signaling events *in vivo* because arterial stiffness increases at sites of vascular injury, and the range of stiffness attained at these injury sites is similar to those that support Rac activation and cell cycling on hydrogels (13). We found that smooth muscle-specific deletion of *Rac1* inhibited neointima formation and smooth muscle cell proliferation after vascular injury *in vivo*. Moreover, among the cell cycle genes that were differentially expressed during the vascular injury response, only cyclin D1 was also downstream of FAK and Rac. We conclude that the FAK-Cas-Rac signaling module is at the core of intracellular stiffening and stiffness-sensitive cell cycling.

## MATERIALS AND METHODS

### Cell culture, siRNA transfection, and adenovirus infection

Spontaneously immortalized mouse embryo fibroblasts (MEFs), primary mouse VSMCs, Cas-mutant MEFs, and SYF-null MEFs were cultured as previously described (13, 63). Cas-null and Cas-mutant MEFs were generously provided by Amy Bouton (University of Virginia) and Steven Hanks (Vanderbilt University). SYF-null (MEFs deficient in Src, Yes, and Fyn) and c-Src-reconstituted SYF-MEFs were purchased from ATCC. Primary mouse VSMCs were isolated by explant culture from 8–10 week old male C57BL/6J mice as described (64). To synchronize MEFs and VSMCs in G0, near-confluent cells were serum-starved by incubation in DMEM with 1 mg/ml heat-inactivated fatty-acid free BSA for 48 hours. The serum-starved cells were trypsinized, centrifuged, and resuspended in serum-free DMEM for 30 minutes at 37°C. Then, cells were replated on fibronectin-coated hydrogels with fresh growth medium (13, 63) containing 10% FBS.

In some experiments, cells were plated in the presence of 0.03  $\mu\text{M}$  jasplakinolide (Calbiochem) or 0.5  $\mu\text{M}$  latrunculin B (Calbiochem) with 10% FBS. For FAK or Rac pharmacologic inhibitor experiments, near confluent MEFs in 35-mm culture dishes were serum-starved for ~48 hours and then stimulated with 10% FBS and either (vehicle), 20  $\mu\text{M}$  FAK inhibitor (PF573228; Tocris Bioscience), or 150  $\mu\text{M}$  Rac inhibitor (NSC23766; Santa Cruz) for selected times up to 20 hours. Although previous publications have used lower doses of these inhibitors (65, 66), we used dose response curves for FAK autophosphorylation and Rac-GTP loading, respectively, in MEFs to select the concentrations of PF573228 and NSC23766 used in our experiments (Fig. S8A–B). PF573228 was dissolved in DMSO as a 750 $\times$  stock; vehicle- and PF573228-treated cells contained the same amounts of DMSO.

siRNA transfections for both MEFs and VSMCs were performed as described with Lipofectamine 2000 (63) in OPTI-MEM using final siRNA concentrations of 150–200 nM. After 4–5 hours of siRNA transfection, cells were allowed to recover overnight in fresh DMEM containing 10% FBS and then serum-starved in BSA-containing DMEM for 48 hours. All siRNA-based experiments were performed 72 hours after transfection. A non-specific Control Duplex X siRNA (target sequence: 5'NNATTCTATCACTAGCGTGAC-3') was used as control (Dharmacon). Adenoviruses were titred and used as described (63). FRNK, FAK<sup>397F</sup>, and Rac<sup>V12</sup> were generous gifts from Christopher Chen (Boston University). Adenoviruses were used at the following multiplicities of infection: FRNK (600), FAK<sup>397F</sup> (1500), wild-type FAK (300), Rac<sup>V12</sup> (900), Rac<sup>N17</sup> (100) and Cyclin D1 (300). Adenoviruses encoding LacZ or GFP were used as controls.

### Preparation of polyacrylamide hydrogels

The detailed protocol for generating fibronectin-coated polyacrylamide hydrogels has been previously described (63, 67). Low (2–4 kPa), medium (10–12 kPa), and high (20–24 kPa) stiffness hydrogels were used for experiments. Different sizes of glass coverslips and cell numbers were used for specific experiments: immunoblotting and Rac activity assay (40-mm,  $2 \times 10^5$  cells), RT-qPCR (25-mm,  $10^5$  cells), EdU incorporation (18-mm,  $4.5 \times 10^4$  cells), and immunostaining (12-mm,  $2 \times 10^4$  cells). Hydrogel volumes were: 500, 150, 33, and 10  $\mu$ l for 40-, 25-, 18-, and 12-mm coverslips, respectively.

### Protein extraction, immunoblotting, and immunostaining

Unless stated otherwise, total cell lysates were prepared from cells cultured on hydrogels by placing the coverslips face-down on 5 $\times$  sample buffer (250 mM Tris pH 6.8, 10% SDS, 50% glycerol, 0.02% bromophenol blue, 10 mM 2-mercaptoethanol) and incubating for 1–2 minutes at room temperature. Equal amounts of extracted protein were fractionated on reducing 10% SDS-polyacrylamide gels, and the fractionated proteins were transferred electrophoretically to nitrocellulose filters. Filters were probed with antibodies to: FAK, Cas, paxillin, vinculin, tubulin, Src, Rac1, cyclin A, cyclin D1, lamellipodin, GAPDH, CrkI, CrkII, DOCK180, phospho-FAK<sup>Tyr576</sup>, phospho-FAK<sup>Tyr397</sup>, phospho-FAK<sup>Tyr576</sup>, phospho-FAK<sup>Tyr861</sup>, phospho-Cas<sup>Tyr410</sup>, phospho-Src<sup>Tyr416</sup>, phospho-Src<sup>Tyr527</sup>, phospho-paxillin<sup>Tyr118</sup>, phospho-vinculin<sup>Tyr822</sup>, or phospho-CrkII<sup>Tyr221</sup>.

For focal adhesion immunostaining, MEFs on hydrogels were fixed in 3.7% formaldehyde for 1 hour, permeabilized with 0.4% Triton X-100 for 30 min, and then blocked in 2% BSA and 0.2% Triton X-100 for 1 hour at room temperature. After incubating with the primary antibodies (paxillin and vinculin) for 2 hours at room temperature, cells were washed three times with PBS containing 2% BSA and 0.2% Triton X-100 and then incubated with either Alexa Fluor 488-conjugated goat anti-rabbit or Alexa Fluor 594-conjugated goat anti-mouse antibodies (Invitrogen) for 1 hour at room temperature. Finally, cells were washed three times with PBS containing 2% BSA and 0.2% Triton X-100 and then once with distilled water before mounting for microscopy. Fluorescence images of cells were acquired as 1- $\mu$ m optical sections with a 40 $\times$ /1.2 water-immersion objective on a Zeiss LSM 510 META/NLO confocal microscope.

### EdU incorporation assay

Serum-starved cells were replated on fibronectin-coated hydrogels with fresh growth medium containing 10% FBS. To assess DNA synthesis, cells were incubated with 10  $\mu$ M 5-ethynyl-2'-deoxyuridine (EdU) (Invitrogen) for 20 hours in the presence of 10% FBS in DMEM. EdU was visualized using the Click-iT EdU Imaging Kit (Invitrogen) according to the manufacturer's instructions. Nuclei were stained with DAPI, and coverslips were mounted onto glass microscope slides. Approximate 4–6 fields of view were counted per sample to determine the percentage of EdU-positive cells relative to DAPI-stained nuclei.

### Rac activity assay

Active Rac GTP was measured using a G-LISA small G-protein activation assay kit (Cytoskeleton) according to manufacturer's directions. Briefly, serum-starved MEFs were replated on fibronectin-coated low- and high-stiffness hydrogels and stimulated with 10% FBS for 1–9 hours. Total cell lysates were prepared with ice-cold lysis buffer (150  $\mu$ l per 40-mm hydrogel), and the protein concentration was measured by Coomassie binding (Bio-Rad). Equal amounts of protein was added to each well of a G-LISA plate and incubated for 30 minutes at 4°C. The bound Rac was detected by adding an anti-Rac primary antibody (45 minutes) and a secondary HRP-labeled antibody (45 minutes) to the each well. Finally, HRP detection reagents were added, and the resulting colorimetric reaction was quantified by measuring absorbance at 490 nm in a microplate spectrophotometer.

### Measurement of intracellular stiffness by AFM

For quantitative measurements of intracellular stiffness, cells were plated on fibronectin-coated low or high stiffness hydrogels in 10% FBS-containing DMEM (phenol red-free). AFM in force mode or force-volume mode was used to monitor the intracellular stiffness of single adherent cells on hydrogels using a DAFM-2X Bioscope (Veeco, Woodbury, NY) mounted on an Axiovert 100 microscope (Zeiss, Thornwood, NY). Cells were indented with a standard silicon nitride cantilever (spring constant =0.06 N/m) with a conical tip (40 nm in diameter). To quantify the cellular stiffness (E; Young's modulus), the first 400 nm of tip deflection from the horizontal was fit with the Hertz model for a cone (68). For each experiment, 5–10 measurements of intracellular stiffness were collected near the periphery of each cell, and each experiment analyzed 8–10 cells per condition. AFM force curves were analyzed and converted to Young's modulus using custom MATLAB scripts generously provided by Paul Janmey. Results from whole cell force-volume maps are representative of 7 (low stiffness) or 8 (high stiffness) cells.

### Bioinformatic Analysis

Global gene expression in microdissected sites of injured femoral arteries of SMA-GFP mice (13, 63) was compared to the genes expressed in the contralateral uninjured arteries. These data have been deposited in GEO as GSE40637. We performed a 2-class paired analysis of the data using Statistical Analysis of Microarray (SAM), uploaded the SAM results into Ingenuity Pathway Analysis, and imposed cutoffs of 1.7 as the minimum fold change and 5% as the minimum false discovery rate (q-value). These criteria yielded 1498 analysis ready molecules, which were compared to the 2019 genes in the "Cell Cycle"

functional grouping within Ingenuity Pathway Analysis. The 281 genes (Table S1) common to both data sets were analyzed using the Path Explorer Tool to identify the subset downstream of FAK (PTK2), Rac1, or both.

### In vivo vascular injury

Rac1<sup>fl/fl</sup> mice on a C57BL/6 background were mated to a smooth-muscle specific, tamoxifen-inducible transgenic Cre line ((69); hereafter called SM-iCre) to obtain progeny with a Rac1<sup>fl/fl</sup>;SM-iCre genotype. Male Rac1<sup>fl/fl</sup>;SM-iCre mice on a chow diet (3 or 4 months old) were given tamoxifen (4 mg in 0.2 ml 98% corn oil, 2% EtOH) or an equivalent volume of vehicle by oral gavage for 5 consecutive days and allowed to recover for 10–14 days. Fine wire femoral artery injury was performed as described (70, 71). To measure in vivo cycling, the mice were given EdU (200 µg in 1.5 ml PBS) *i.p.*, divided equally over three injections given at 72, 48, and 24 hours before sacrifice. The mice were sacrificed 14 days after wire injury. The injured artery and uninjured contralateral control were fixed in Prefer (Anatech), isolated, embedded in paraffin, sliced into 6-µm sections, and stained for elastin (Accustain Elastin Stain; Sigma-Aldrich) or incorporated EdU (Invitrogen) following the manufacturer's recommendations. For cyclin D1 immunohistochemical staining, paraffin sections were blocked with power block buffer (BioGenex Laboratories), incubated with anti-cyclin D1 (1:200 dilution; Thermo Scientific) overnight at 4°C, and washed in PBS followed by a 2-hour incubation with biotinylated goat anti-rabbit IgG (1:200 dilution; Vector Lab). Vectastain ABC (Vector Laboratories) and DAB (Dako) were used to detect cyclin D1. Immunostaining with anti-Rac 1 (1:100 dilution; Santa Cruz), anti-Cas (1:100 dilution; BD Transduction Laboratories), and anti-phospho-Cas (1:100 dilution; Sigma) was performed in sections blocked with 2% BSA in 0.1 M Tris-HCl, pH 7.5. Primary antibodies were incubated overnight at 4°C, washed in 0.1 M Tris-HCl, pH 7.5 and then incubated with Alexa Fluor 488-conjugated goat anti-rabbit (phosphoCas) or Alexa Fluor 594-conjugated goat anti-mouse (Rac1) antibodies (1:100 dilution; Life Technology) secondary antibodies for 1 hour at room temperature. The section were washed as above and mounted in Fluoromount-G (Southern Biotech) Images were captured at 20× magnification using a Nikon Eclipse 80i microscope equipped with a Hamamatsu C4742-95 digital camera and camera controller with ImagePro software (Media Cybernetics). Mouse procedures were approved by the University of Pennsylvania Institutional Animal Care and Use Committee.

### Statistical analysis

In vitro data are presented as means ± SD of the indicated number of independent experiments. Data were analyzed with a Mann-Whitney test. In vivo data are presented as Tukey box and whisker plots and analyzed with a Mann-Whitney test. *p* values < 0.05 were considered to be statistically significant.

### ACKNOWLEDGEMENTS

We thank Victor Tybulewicz (National Institute of Medical Research, London) for the floxed Rac1 mice, and Stefan Offermanns (Max Planck Institute for Heart and Lung Research) for the smooth muscle-specific, inducible Cre mouse. Cas-null and Cas-mutant MEFs were generously provided by Amy Bouton (University of Virginia) and Steven Hanks (Vanderbilt University). Paul Janmey (University of Pennsylvania) generously provided the MATLAB Script for AFM analysis. Chis Chen (Boston University) provided several adenoviruses. The bioinformatics and confocal analyses were performed with assistance from John Tobias at the Molecular Profiling

facility and Xinyu Zhao at the Microscopy Core facility, respectively. We thank Kathleen Probert (University of Pennsylvania) for advising us on the statistical analysis. We thank Jongsik Kim (University of Illinois at Urbana-Champaign) for technical supports on generating the 3D height and force-maps. **FUNDING:** This work was supported by NIH grants HL094491, HL093283, and HL62250. Y.H.B. and Z.R. were supported by a post-doctoral fellowship from the American Heart Association. A.C. and Z.R. were supported by NIH training grant T32 HL007954. K.L.M. was supported by NIH training grant R25CA101871.

## REFERENCES AND NOTES

1. Pelham RJ, Wang Y-I. Cell locomotion and focal adhesions are regulated by substrate flexibility. *Proceedings of the National Academy of Sciences*. 1997; 94:13661–13665.
2. Paszek M, Weaver V. The Tension Mounts: Mechanics Meets Morphogenesis and Malignancy. *Journal of Mammary Gland Biology and Neoplasia*. 2004; 9:325–342. [PubMed: 15838603]
3. Engler AJ, Sen S, Sweeney HL, Discher DE. Matrix Elasticity Directs Stem Cell Lineage Specification. *Cell*. 2006; 126:677–689. [PubMed: 16923388]
4. Provenzano PP, Inman DR, Eliceiri KW, Keely PJ. Matrix density-induced mechanoregulation of breast cell phenotype, signaling and gene expression through a FAK-ERK linkage. *Oncogene*. 2009; 28:4326–4343. [PubMed: 19826415]
5. Kothapalli D, Liu S-L, Bae Yong H, Monslow J, Xu T, Hawthorne Elizabeth A, Byfield Fitzroy J, Castagnino P, Rao S, Rader Daniel J, Pure E, Phillips Michael C, Lund-Katz S, Janmey Paul A, Assoian Richard K. Cardiovascular Protection by ApoE and ApoE-HDL Linked to Suppression of ECM Gene Expression and Arterial Stiffening. *Cell Reports*. 2012; 2:1259–1271. [PubMed: 23103162]
6. Schrader J, Gordon-Walker TT, Aucott RL, van Deemter M, Quaas A, Walsh S, Benten D, Forbes SJ, Wells RG, Iredale JP. Matrix stiffness modulates proliferation, chemotherapeutic response, and dormancy in hepatocellular carcinoma cells. *Hepatology*. 2011; 53:1192–1205. [PubMed: 21442631]
7. Paszek MJ, Zahir N, Johnson KR, Lakins JN, Rozenberg GI, Gefen A, Reinhart-King CA, Margulies SS, Dembo M, Boettiger D, Hammer DA, Weaver VM. Tensional homeostasis and the malignant phenotype. *Cancer Cell*. 2005; 8:241–254. [PubMed: 16169468]
8. Owen KA, Abshire MY, Tilghman RW, Casanova JE, Bouton AH. FAK Regulates Intestinal Epithelial Cell Survival and Proliferation during Mucosal Wound Healing. *PLoS ONE*. 2011; 6:e23123. [PubMed: 21887232]
9. Butcher DT, Alliston T, Weaver VM. A tense situation: forcing tumour progression. *Nat Rev Cancer*. 2009; 9:108–122. [PubMed: 19165226]
10. Friedland JC, Lee MH, Boettiger D. Mechanically Activated Integrin Switch Controls  $\alpha 5 \beta 1$  Function. *Science*. 2009; 323:642–644. [PubMed: 19179533]
11. Yeung T, Georges PC, Flanagan LA, Marg B, Ortiz M, Funaki M, Zahir N, Ming W, Weaver V, Janmey PA. Effects of substrate stiffness on cell morphology, cytoskeletal structure, and adhesion. *Cell Motility and the Cytoskeleton*. 2005; 60:24–34. [PubMed: 15573414]
12. Burridge K, Wittchen ES. The tension mounts: Stress fibers as force-generating mechanotransducers. *The Journal of Cell Biology*. 2013; 200:9–19. [PubMed: 23295347]
13. Klein EA, Yin L, Kothapalli D, Castagnino P, Byfield FJ, Xu T, Levental I, Hawthorne E, Janmey PA, Assoian RK. Cell-Cycle Control by Physiological Matrix Elasticity and In Vivo Tissue Stiffening. *Current Biology*. 2009; 19:1511–1518. [PubMed: 19765988]
14. Sastry SK, Burridge K. Focal Adhesions: A Nexus for Intracellular Signaling and Cytoskeletal Dynamics. *Experimental Cell Research*. 2000; 261:25–36. [PubMed: 11082272]
15. Dumbauld DW, Lee TT, Singh A, Scrimgeour J, Gersbach CA, Zamir EA, Fu J, Chen CS, Curtis JE, Craig SW, Garcia AJ. How vinculin regulates force transmission. *Proceedings of the National Academy of Sciences*. 2013; 110:9788–9793.
16. Fabry B, Klemm H, Kienle S, Schaffer Tilman E, Goldmann Wolfgang H. Focal Adhesion Kinase Stabilizes the Cytoskeleton. *Biophysical Journal*. 2011; 101:2131–2138. [PubMed: 22067150]
17. Sawada Y, Tamada M, Dubin-Thaler BJ, Cherniavskaya O, Sakai R, Tanaka S, Sheetz MP. Force Sensing by Mechanical Extension of the Src Family Kinase Substrate p130Cas. *Cell*. 2006; 127:1015–1026. [PubMed: 17129785]

18. Grashoff C, Hoffman BD, Brenner MD, Zhou R, Parsons M, Yang MT, McLean MA, Sligar SG, Chen CS, Ha T, Schwartz MA. Measuring mechanical tension across vinculin reveals regulation of focal adhesion dynamics. *Nature*. 2010; 466:263–266. [PubMed: 20613844]
19. Kostic A, Sheetz MP. Fibronectin Rigidity Response through Fyn and p130Cas Recruitment to the Leading Edge. *Molecular Biology of the Cell*. 2006; 17:2684–2695. [PubMed: 16597701]
20. Plotnikov, Sergey V.; Pasapera, Ana M.; Sabass, B. Clare M. Waterman, Force Fluctuations within Focal Adhesions Mediate ECM-Rigidity Sensing to Guide Directed Cell Migration. *Cell*. 2012; 151:1513–1527. [PubMed: 23260139]
21. Hoffman BD, Grashoff C, Schwartz MA. Dynamic molecular processes mediate cellular mechanotransduction. *Nature*. 2011; 475:316–323. [PubMed: 21776077]
22. Pasapera AM, Schneider IC, Rericha E, Schlaepfer DD, Waterman CM. Myosin II activity regulates vinculin recruitment to focal adhesions through FAK-mediated paxillin phosphorylation. *The Journal of Cell Biology*. 2010; 188:877–890. [PubMed: 20308429]
23. Fonseca PM, Shin N-Y, Brabek J, Ryzhova L, Wu J, Hanks SK. Regulation and localization of CAS substrate domain tyrosine phosphorylation. *Cellular Signalling*. 2004; 16:621–629. [PubMed: 14751547]
24. Ruest PJ, Shin N-Y, Polte TR, Zhang X, Hanks SK. Mechanisms of CAS Substrate Domain Tyrosine Phosphorylation by FAK and Src. *Molecular and cellular biology*. 2001; 21:7641–7652. [PubMed: 11604500]
25. Defilippi P, Di Stefano P, Cabodi S. p130Cas: a versatile scaffold in signaling networks. *Trends in Cell Biology*. 2006; 16:257–263. [PubMed: 16581250]
26. Turner CE. Paxillin and focal adhesion signalling. *Nat Cell Biol*. 2000; 2:E231–E236. [PubMed: 11146675]
27. Burrige K, Turner CE, Romer LH. Tyrosine phosphorylation of paxillin and pp125FAK accompanies cell adhesion to extracellular matrix: a role in cytoskeletal assembly. *The Journal of Cell Biology*. 1992; 119:893–903. [PubMed: 1385444]
28. Subauste MC, Pertz O, Adamson ED, Turner CE, Junger S, Hahn KM. Vinculin modulation of paxillin–FAK interactions regulates ERK to control survival and motility. *The Journal of Cell Biology*. 2004; 165:371–381. [PubMed: 15138291]
29. Ballestrem C, Erez N, Kirchner J, Kam Z, Bershadsky A, Geiger B. Molecular mapping of tyrosine-phosphorylated proteins in focal adhesions using fluorescence resonance energy transfer. *Journal of Cell Science*. 2006; 119:866–875. [PubMed: 16478788]
30. Janoštiak R, Tolde O, Br hova Z, Novotný M, Hanks SK, Rösel D, Brábek J. Tyrosine phosphorylation within the SH3 domain regulates CAS subcellular localization, cell migration, and invasiveness. *Molecular Biology of the Cell*. 2011; 22:4256–4267. [PubMed: 21937722]
31. Mitra SK, Schlaepfer DD. Integrin-regulated FAK–Src signaling in normal and cancer cells. *Current Opinion in Cell Biology*. 2006; 18:516–523. [PubMed: 16919435]
32. Schaller MD, Hildebrand JD, Shannon JD, Fox JW, Vines RR, Parsons JT. Autophosphorylation of the focal adhesion kinase, pp125FAK, directs SH2-dependent binding of pp60src. *Molecular and cellular biology*. 1994; 14:1680–1688. [PubMed: 7509446]
33. Kjölller L, Hall A. Rac Mediates Cytoskeletal Rearrangements and Increased Cell Motility Induced by Urokinase-Type Plasminogen Activator Receptor Binding to Vitronectin. *The Journal of Cell Biology*. 2001; 152:1145–1158. [PubMed: 11257116]
34. Van Aelst L, D’Souza-Schorey C. Rho GTPases and signaling networks. *Genes & Development*. 1997; 11:2295–2322. [PubMed: 9308960]
35. Ridley AJ, Hall A. The small GTP-binding protein rho regulates the assembly of focal adhesions and actin stress fibers in response to growth factors. *Cell*. 1992; 70:389–399. [PubMed: 1643657]
36. Nobes CD, Hall A. Rho, Rac, and Cdc42 GTPases regulate the assembly of multimolecular focal complexes associated with actin stress fibers, lamellipodia, and filopodia. *Cell*. 1995; 81:53–62. [PubMed: 7536630]
37. Hall A. Rho GTPases and the Actin Cytoskeleton. *Science*. 1998; 279:509–514. [PubMed: 9438836]
38. Schoenwaelder SM, Burrige K. Bidirectional signaling between the cytoskeleton and integrins. *Current Opinion in Cell Biology*. 1999; 11:274–286. [PubMed: 10209151]

39. Cho SY, Klemke RL. Purification of pseudopodia from polarized cells reveals redistribution and activation of Rac through assembly of a CAS/Crk scaffold. *The Journal of Cell Biology*. 2002; 156:725–736. [PubMed: 11839772]
40. Kiyokawa E, Hashimoto Y, Kobayashi S, Sugimura H, Kurata T, Matsuda M. Activation of Rac1 by a Crk SH3-binding protein, DOCK180. *Genes & Development*. 1998; 12:3331–3336. [PubMed: 9808620]
41. Hsia DA, Mitra SK, Hauck CR, Streblov DN, Nelson JA, Ilic D, Huang S, Li E, Nemerow GR, Leng J, Spencer KSR, Cheresch DA, Schlaepfer DD. Differential regulation of cell motility and invasion by FAK. *The Journal of Cell Biology*. 2003; 160:753–767. [PubMed: 12615911]
42. Klein EA, Campbell LE, Kothapalli D, Fournier AK, Assoian RK. Joint Requirement for Rac and ERK Activities Underlies the Mid-G1 Phase Induction of Cyclin D1 and S Phase Entry in Both Epithelial and Mesenchymal Cells. *Journal of Biological Chemistry*. 2008; 283:30911–30918. [PubMed: 18715870]
43. Assoian RK, Schwartz MA. Coordinate signaling by integrins and receptor tyrosine kinases in the regulation of G1 phase cell-cycle progression. *Current Opinion in Genetics & Development*. 2001; 11:48–53. [PubMed: 11163150]
44. Joyce D, Bouzahzah B, Fu M, Albanese C, D'Amico M, Steer J, Klein JU, Lee RJ, Segall JE, Westwick JK, Der CJ, Pestell RG. Integration of Rac-dependent Regulation of Cyclin D1 Transcription through a Nuclear Factor- $\kappa$ B-dependent Pathway. *Journal of Biological Chemistry*. 1999; 274:25245–25249. [PubMed: 10464245]
45. Bubb MR, Spector I, Beyer BB, Fosen KM. Effects of Jasplakinolide on the Kinetics of Actin Polymerization: an explanation for certain in vivo observations. *Journal of Biological Chemistry*. 2000; 275:5163–5170. [PubMed: 10671562]
46. Thyberg J, Blomgren K, Roy J, Tran PK, Hedin U. Phenotypic Modulation of Smooth Muscle Cells after Arterial Injury Is Associated with Changes in the Distribution of Laminin and Fibronectin. *Journal of Histochemistry & Cytochemistry*. 1997; 45:837–846. [PubMed: 9199669]
47. Thyberg J, Hedin U, Sjölund M, Palmberg L, Bottger BA. Regulation of differentiated properties and proliferation of arterial smooth muscle cells. *Arteriosclerosis, Thrombosis, and Vascular Biology*. 1990; 10:966–990.
48. Krause M, Leslie JD, Stewart M, Lafuente EM, Valderrama F, Jagannathan R, Strasser GA, Rubinson DA, Liu H, Way M, Yaffe MB, Boussiotis VA, Gertler FB. Lamellipodin, an Ena/VASP Ligand, Is Implicated in the Regulation of Lamellipodial Dynamics. *Developmental Cell*. 2004; 7:571–583. [PubMed: 15469845]
49. Krause M, Dent EW, Bear JE, Loureiro JJ, Gertler FB. Ena/VASP proteins: regulators of the actin cytoskeleton and cell migration. *Annual review of cell and developmental biology*. 2003; 19:541–564.
50. Bae YH, Ding Z, Zou L, Wells A, Gertler F, Roy P. Loss of profilin-1 expression enhances breast cancer cell motility by Ena/VASP proteins. *Journal of Cellular Physiology*. 2009; 219:354–364. [PubMed: 19115233]
51. Law A-L, Vehlow A, Kotini M, Dodgson L, Soong D, Theveneau E, Bodo C, Taylor E, Navarro C, Perera U, Michael M, Dunn GA, Bennett D, Mayor R, Krause M. Lamellipodin and the Scar/WAVE complex cooperate to promote cell migration in vivo. *The Journal of Cell Biology*. 2013; 203:673–689. [PubMed: 24247431]
52. Insall RH, Machesky LM. Actin Dynamics at the Leading Edge: From Simple Machinery to Complex Networks. *Developmental Cell*. 2009; 17:310–322. [PubMed: 19758556]
53. Campellone KG, Welch MD. A nucleator arms race: cellular control of actin assembly. *Nat Rev Mol Cell Biol*. 2010; 11:237–251. [PubMed: 20237478]
54. Chen Y, Pasapera AM, Koretsky AP, Waterman CM. Orientation-specific responses to sustained uniaxial stretching in focal adhesion growth and turnover. *Proceedings of the National Academy of Sciences*. 2013; 110:E2352–E2361.
55. Hildebrand JD, Taylor JM, Parsons JT. An SH3 domain-containing GTPase-activating protein for Rho and Cdc42 associates with focal adhesion kinase. *Molecular and cellular biology*. 1996; 16:3169–3178. [PubMed: 8649427]

56. Cen B, Selvaraj A, Burgess RC, Hitzler JK, Ma Z, Morris SW, Prywes R. Megakaryoblastic Leukemia 1, a Potent Transcriptional Coactivator for Serum Response Factor (SRF), Is Required for Serum Induction of SRF Target Genes. *Molecular and cellular biology*. 2003; 23:6597–6608. [PubMed: 12944485]
57. Miralles F, Posern G, Zaromytidou A-I, Treisman R. Actin Dynamics Control SRF Activity by Regulation of Its Coactivator MAL. *Cell*. 2003; 113:329–342. [PubMed: 12732141]
58. Baarlink C, Wang H, Grosse R. Nuclear Actin Network Assembly by Formins Regulates the SRF Coactivator MAL. *Science*. 2013; 340:864–867. [PubMed: 23558171]
59. Medjkane S, Perez-Sanchez C, Gaggioli C, Sahai E, Treisman R. Myocardin-related transcription factors and SRF are required for cytoskeletal dynamics and experimental metastasis. *Nat Cell Biol*. 2009; 11:257–268. [PubMed: 19198601]
60. Lyulcheva E, Taylor E, Michael M, Vehlou A, Tan S, Fletcher A, Krause M, Bennett D. Drosophila Pico and Its Mammalian Ortholog Lamellipodin Activate Serum Response Factor and Promote Cell Proliferation. *Developmental Cell*. 2008; 15:680–690. [PubMed: 19000833]
61. Dupont S, Morsut L, Aragona M, Enzo E, Giulitti S, Cordenonsi M, Zanconato F, Le Digabel J, Forcato M, Bicciato S, Elvassore N, Piccolo S. Role of YAP/TAZ in mechanotransduction. *Nature*. 2011; 474:179–183. [PubMed: 21654799]
62. Aragona M, Panciera T, Manfrin A, Giulitti S, Michielin F, Elvassore N, Dupont S, Piccolo S. A Mechanical Checkpoint Controls Multicellular Growth through YAP/TAZ Regulation by Actin-Processing Factors. *Cell*. 2013; 154:1047–1059. [PubMed: 23954413]
63. Klein, EA.; Yung, Y.; Castagnino, P.; Kothapalli, D.; Assoian, RK. *Methods in Enzymology*. David, AC., editor. Vol. 426. Academic Press; 2007. p. 155-175.
64. Cuff CA, Kothapalli D, Azonobi I, Chun S, Zhang Y, Belkin R, Yeh C, Secreto A, Assoian RK, Rader DJ, Ellen Pur xE. The adhesion receptor CD44 promotes atherosclerosis by mediating inflammatory cell recruitment and vascular cell activation. *The Journal of Clinical Investigation*. 2001; 108:1031–1040. [PubMed: 11581304]
65. Slack-Davis JK, Martin KH, Tilghman RW, Iwanicki M, Ung EJ, Autry C, Luzzio MJ, Cooper B, Kath JC, Roberts WG, Parsons JT. Cellular Characterization of a Novel Focal Adhesion Kinase Inhibitor. *Journal of Biological Chemistry*. 2007; 282:14845–14852. [PubMed: 17395594]
66. Gao Y, Dickerson JB, Guo F, Zheng J, Zheng Y. Rational design and characterization of a Rac GTPase-specific small molecule inhibitor. *Proceedings of the National Academy of Sciences of the United States of America*. 2004; 101:7618–7623. [PubMed: 15128949]
67. Cretu A, Castagnino P, Assoian R. Studying the Effects of Matrix Stiffness on Cellular Function using Acrylamide-based Hydrogels. 2010:e2089.
68. Domke J, Radmacher M. Measuring the Elastic Properties of Thin Polymer Films with the Atomic Force Microscope. *Langmuir*. 1998; 14:3320–3325.
69. Wirth A, Benyo Z, Lukasova M, Leutgeb B, Wettschureck N, Gorbey S, Orsy P, Horvath B, Maser-Gluth C, Greiner E, Lemmer B, Schutz G, Gutkind JS, Offermanns S. G12–G13-LARG-mediated signaling in vascular smooth muscle is required for salt-induced hypertension. *Nat Med*. 2008; 14:64–68. [PubMed: 18084302]
70. Kothapalli D, Zhao L, Hawthorne EA, Cheng Y, Lee E, Pure E, Assoian RK. Hyaluronan and CD44 antagonize mitogen-dependent cyclin D1 expression in mesenchymal cells. *The Journal of Cell Biology*. 2007; 176:535–544. [PubMed: 17296798]
71. Castagnino P, Kothapalli D, Hawthorne EA, Liu S-L, Xu T, Rao S, Yung Y, Assoian RK. miR-221/222 Compensates for Skp2-Mediated p27 Degradation and Is a Primary Target of Cell Cycle Regulation by Prostacyclin and cAMP. *PLoS ONE*. 2013; 8:e56140. [PubMed: 23409140]

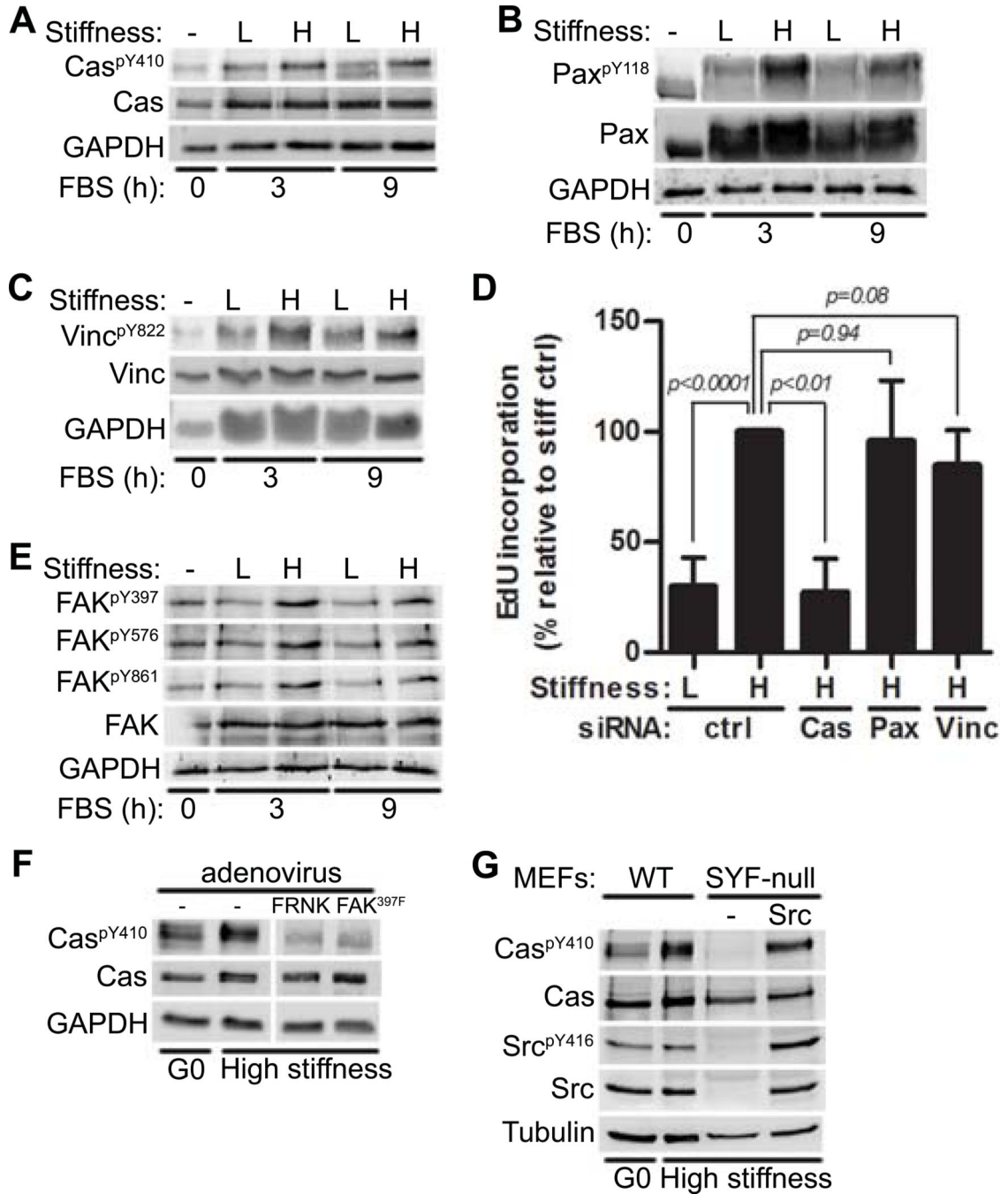


**Figure 1. FAK/Src-mediated Cas phosphorylation transduces ECM stiffness into mechanosensitive cell cycling**

Serum-starved MEFs were incubated on low or high stiffness hydrogels and stimulated with FBS as indicated. Total cell lysates were immunoblotted. (A–C) Lysates analyzed for phosphorylated and total Cas (A), paxillin (B; Pax), or vinculin (C; Vinc). N=3 independent biological replicates for (A) to (C). (D) Starved MEFs transfected with a control (ctrl) siRNA or siRNAs to Cas, paxillin, or vinculin were seeded on high stiffness hydrogels with FBS for 20 hours. S phase entry was assessed by EdU incorporation. Error bars show mean  $\pm$  SD, N=4 independent biological replicates. (E) Same experiment as in (A) but lysates

were probed for Tyr<sup>397</sup>, Tyr<sup>576</sup>, Tyr<sup>861</sup>, and total FAK. (F) Starved MEFs infected with adenoviruses (FRNK or FAK<sup>397F</sup>) were replated on stiff hydrogels with FBS for 9 hours and probed for phosphorylated and total Cas. The vertical white bar indicates removal of irrelevant lanes from a single blot. N=3 independent biological replicates. (G) WT MEFs, SYF-null (MEFs deficient in Src, Yes, and Fyn) and c-Src-reconstituted SYF-MEFs were plated on high stiffness hydrogels and stimulated with FBS for 9 hours. N=3 independent biological replicates for (E) to (G).

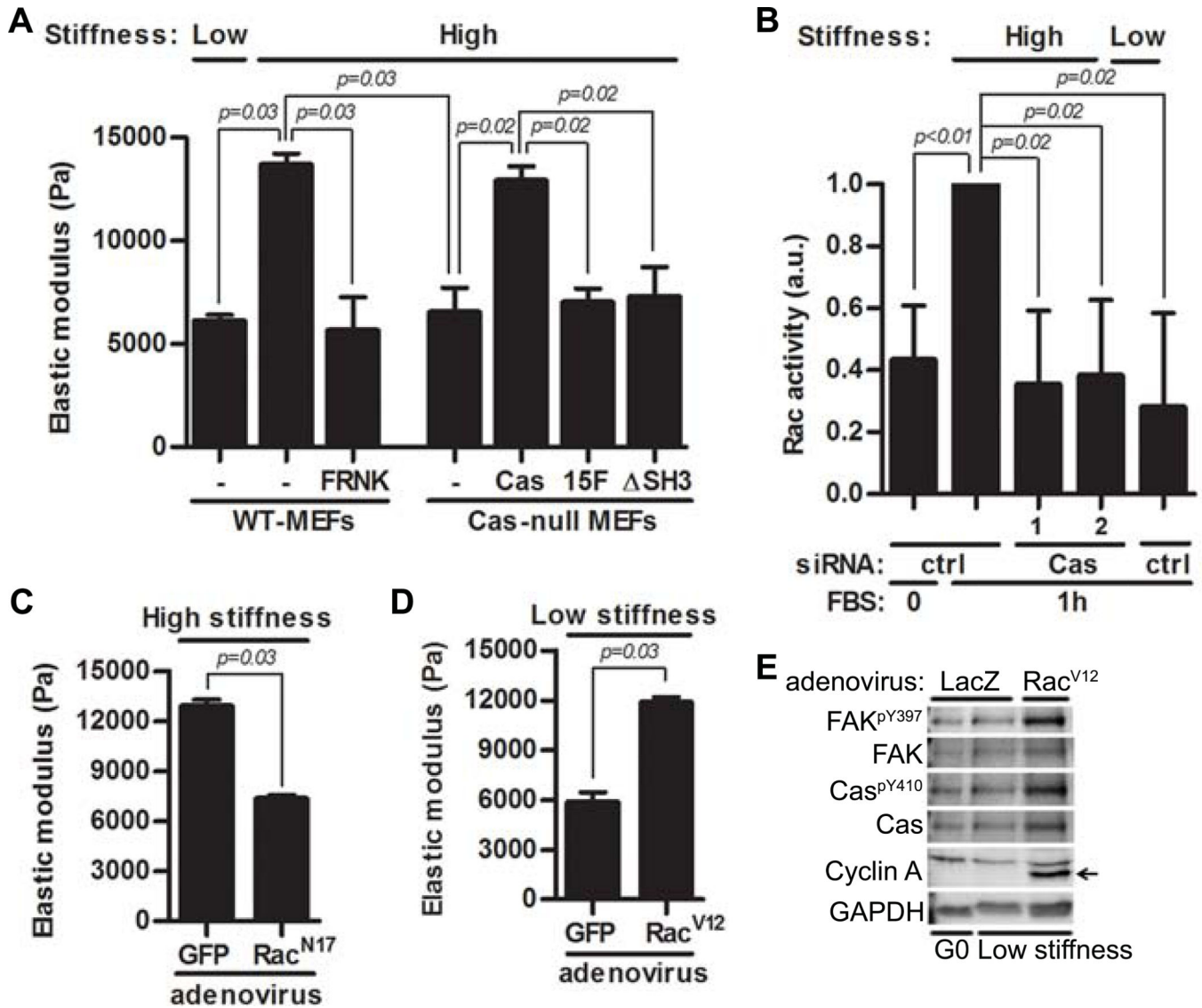


**Figure 2. The FAK-Cas-Rac signaling module transduces substratum stiffness into intracellular stiffness and mechanosensitive cell cycling**

(A) Serum-starved MEFs and Cas-null MEFs, Cas-null MEFs reconstituted with WT-Cas, Cas<sup>15F</sup>, Cas<sup>ΔSH3</sup>, and FAK-inhibited (FRNK) MEFs were cultured on high or low stiffness hydrogels with FBS. Intracellular stiffness was determined by AFM; error bars show mean ± SD, N=4 independent biological replicates. (B) Starved MEFs transfected with a control (ctrl) siRNA or Cas siRNAs were replated on low- or high stiffness hydrogels with FBS. Rac activity was determined by G-LISA; error bars show mean ± SD, N=4 independent biological replicates. (C) Starved MEFs infected with adenoviruses encoding GFP or Rac<sup>N17</sup> were plated on high stiffness hydrogels overnight. Intracellular stiffness was determined by AFM; error bars show mean ± SD, N=4 independent biological replicates. (D) Starved MEFs infected with adenoviruses encoding GFP or Rac<sup>V12</sup> were plated on low stiffness hydrogels with FBS overnight. Intracellular stiffness was determined by AFM; error bars show mean ± SD, N=4 independent biological replicates. (E) Starved MEFs infected with

adenoviruses encoding LacZ or Rac<sup>V12</sup> were plated on low stiffness hydrogels with FBS for 20 hours; lysates were analyzed by immunoblotting. N=3 independent biological replicates.

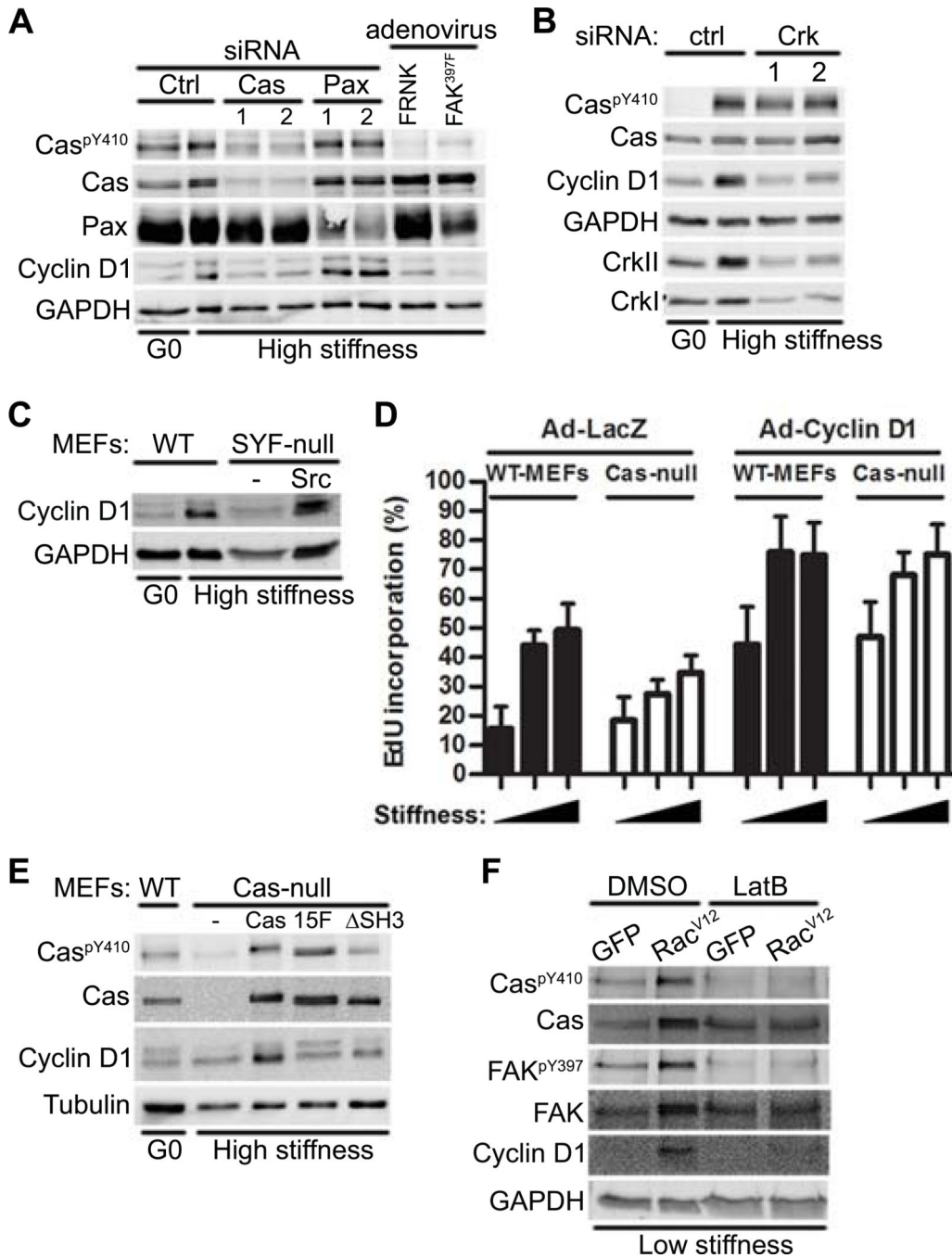


**Figure 3. A FAK-Cas-Rac signaling module is necessary for the mechanosensitive induction of cyclin D1**

(A) Immunoblot of starved MEFs transfected with Cas or paxillin siRNAs or infected with adenoviruses encoding FRNK or FAK<sup>397F</sup> and plated on high or low stiffness hydrogels with FBS for 9 hours. N=3 independent biological replicates. (B) Immunoblot of starved MEFs transfected with control or CrkII siRNAs plated on fibronectin-coated high stiffness hydrogels with FBS for 9 hours. N=3 independent biological replicates. (C) Immunoblot of wild-type MEFs, SYF-null MEFs, and c-Src-reconstituted SYF-MEFs plated on high-stiffness hydrogels with FBS for 9 hours. N=3 independent biological replicates. (D)

Immunoblot of wild-type and Cas-null MEFs that were starved, infected with adenoviruses encoding LacZ or Cyclin D1, and plated on low, medium, or high stiffness fibronectin-coated hydrogels. S phase entry was assessed by EdU incorporation; error bars show mean  $\pm$  SD, N=4 independent biological replicates. (E) Immunoblot of serum-starved wild-type, Cas-null, Cas-reconstituted (Cas), Cas<sup>15F</sup>, and Cas<sup>SH3</sup> MEFs plated on high stiffness hydrogels with FBS for 9 hours. N=3 independent biological replicates. (F) Immunoblot of starved MEFs infected with adenoviruses encoding GFP or Rac<sup>V12</sup> and plated on low stiffness hydrogels with FBS  $\pm$  latrunculin B (LatB) for 9 hours. N=3 independent biological replicates.

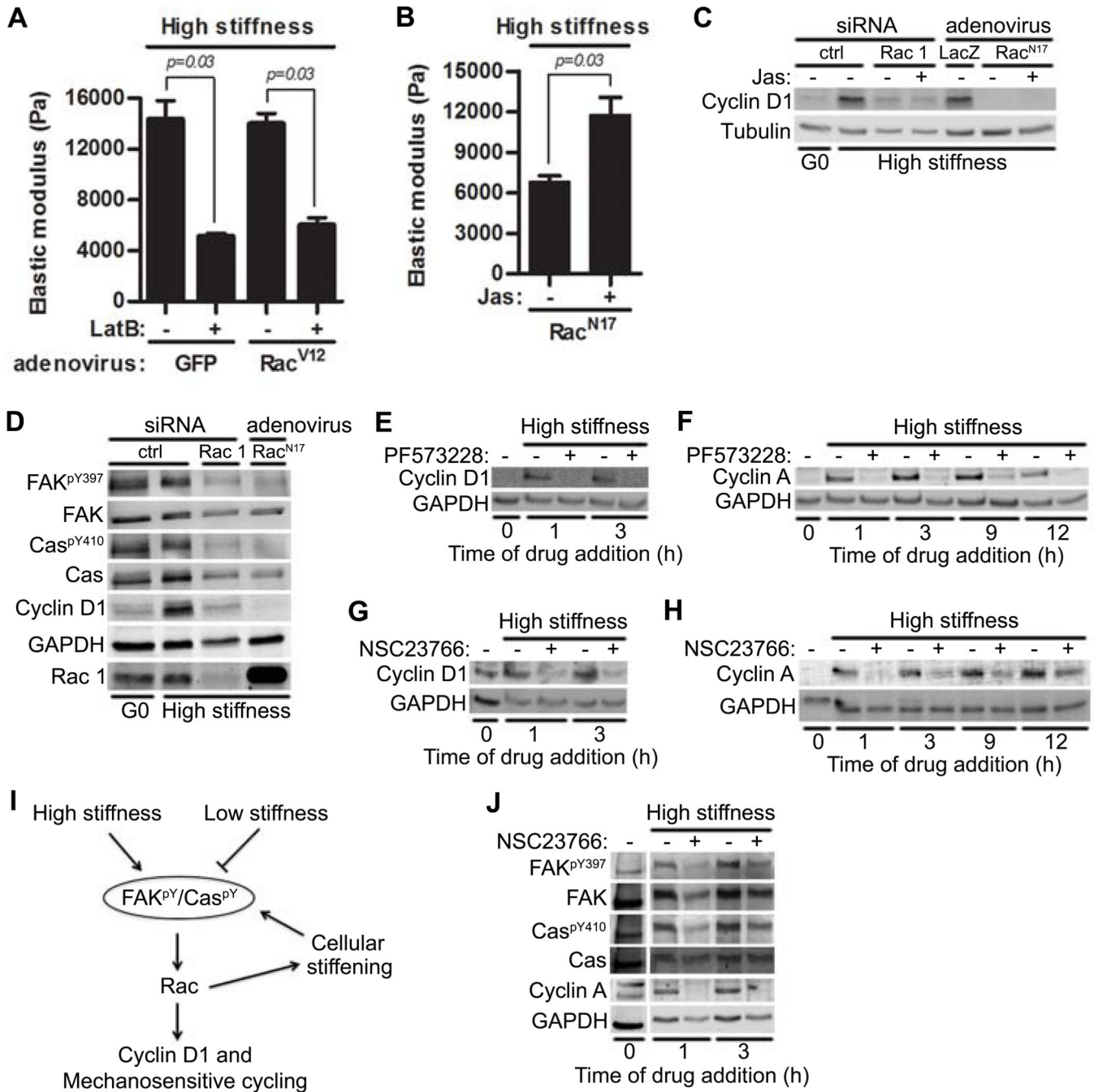


**Figure 4. Rac-dependent intracellular stiffening maintains information flow through the FAK-Cas-Rac signaling pathway**  
 (A) Starved MEFs infected with adenoviruses encoding GFP or Rac<sup>V12</sup> were plated on high stiffness hydrogels with FBS ± latrunculin B (LatB); intracellular stiffness was measured by AFM. Error bars show mean ± SD. N=4 independent biological replicates. (B–C) Starved MEFs were either transfected with control or Rac1 siRNA or infected with adenoviruses encoding LacZ or Rac<sup>N17</sup>. The cells were plated on high stiffness hydrogels with FBS ± jasplakinolide (Jas) and analyzed by AFM (B; error bars show mean ± SD) or immunoblotting (C); N=4 and 3 independent biological replicates for (B) and (C),

NIH-PA Author Manuscript

respectively. (D) Immunoblot of starved MEFs infected with adenovirus encoding Rac<sup>N17</sup> or transfected with control or Rac1 siRNAs. N=3 biological replicates. (E–H) Serum-starved MEFs were plated on high stiffness hydrogels with FBS and treated with the FAK inhibitor PF573228 or the Rac inhibitor NSC23766 at the indicated times. (E and G) Samples were collected after 9 hours, and analyzed by immunoblotting for cyclin D1. N=3 biological replicates. (F and H) The experiment in E and G was repeated except that cells were collected at 20 hours and analyzed for cyclin A. N=3 biological replicates. (I) Model of feed-forward and feed-back mechanotransduction through the FAK-Cas-Rac signaling module. (J) Starved MEFs were seeded on high stiffness hydrogels with FBS and treated with NSC23766 at the indicated times. Lysates were collected at 20 hours (a time when cyclin A would be expressed in cycling cells) and immunoblotted. The vertical white bar indicates removal of irrelevant lanes from a single blot. N=3 independent biological replicates.

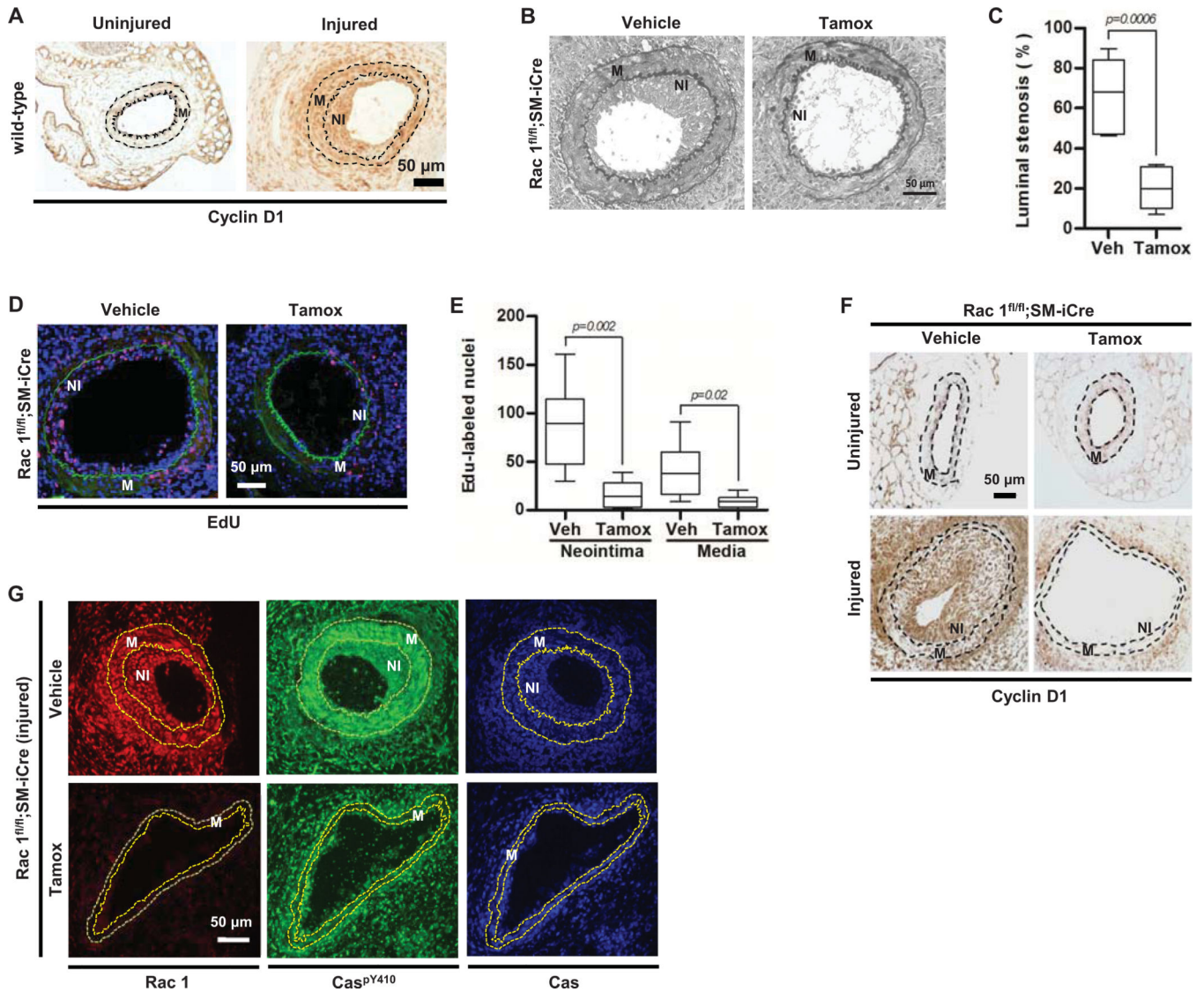


**Figure 5. Rac1 is essential for the proliferative response to vascular injury in vivo and cyclin D1 abundance and Cas phosphorylation are reduced in the vascular smooth muscle cells of Rac-null arteries after injury**

(A) Representative cyclin D1 staining of uninjured and injured femoral artery sections from C57BL/6 mice; N=5. (B) Representative elastin staining of injured femoral artery sections in Rac1<sup>fl/fl</sup>;SM-iCre mice treated with vehicle or tamoxifen (tamox). NI; neointima. M; media. (C) Quantification of the percent luminal stenosis; N=7 mice per genotype and treatment. (D) Representative images of EdU incorporation (red) in injured femoral artery sections of Rac1<sup>fl/fl</sup>;SM-iCre mice treated with vehicle or tamoxifen. DAPI-stained nuclei and elastic lamina are shown in blue and green respectively. (E) Quantification of the EdU response; N=6–7 mice per genotype and treatment. (F) Cyclin D1 staining of uninjured and injured femoral artery sections from Rac1<sup>fl/fl</sup>;SM-iCre mice treated with vehicle or tamoxifen. Images are representative of N=3 (uninjured) or N=6 (injured) mice per genotype and treatment. (G) Rac, Cas<sup>pY410</sup>, and total Cas staining of injured femoral artery sections from Rac1<sup>fl/fl</sup>;SM-iCre mice treated with vehicle or tamoxifen. Images are representative of N=3

mice per genotype and treatment. In (F) and (G), dashed lines show the internal elastic lamina and external elastic laminae. M; media. NI; Neointima. Scale bar = 50  $\mu$ m.

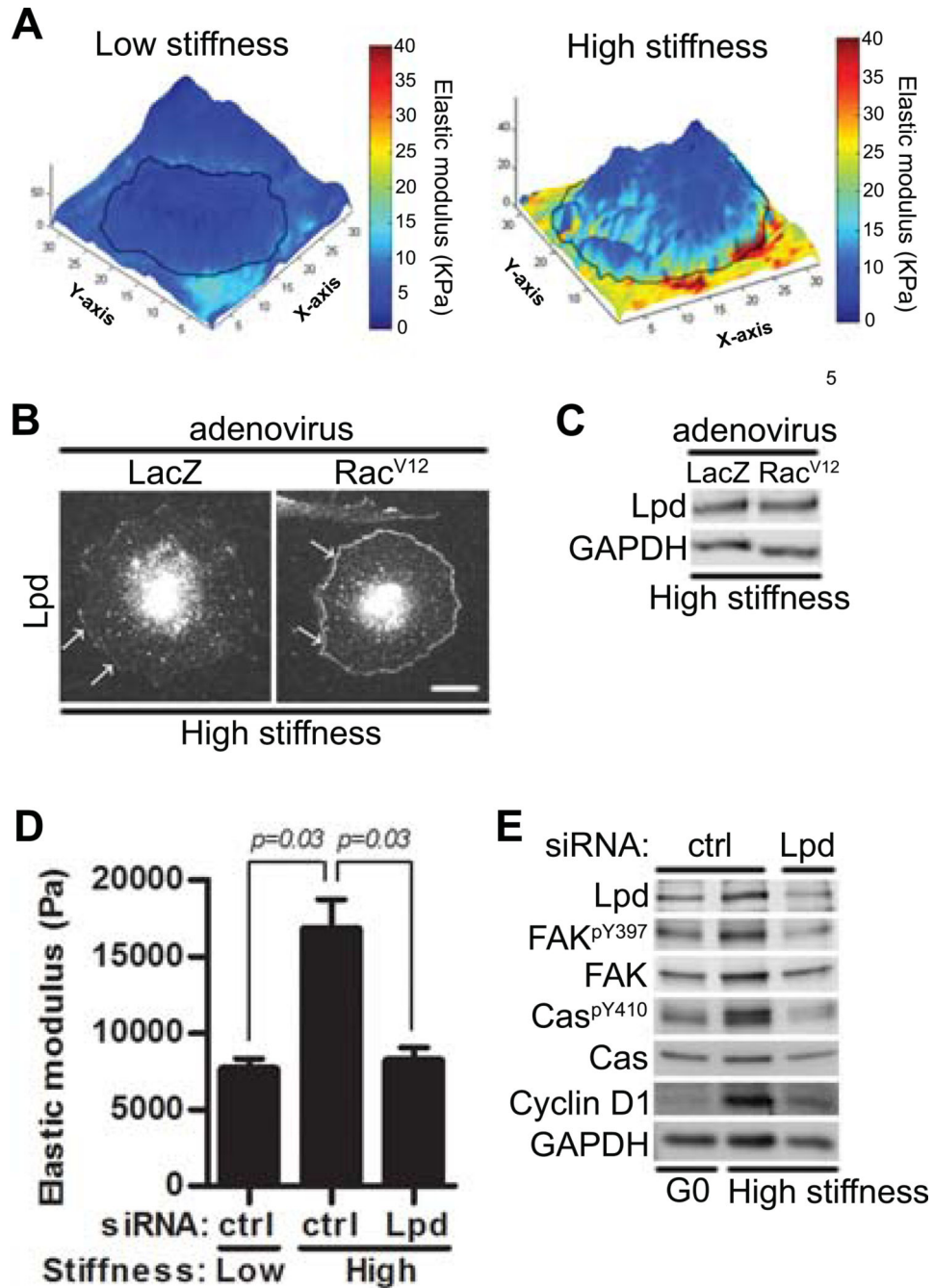


**Figure 6. Lamellipodin links Rac to intracellular stiffening and cell cycling**

(A) Starved MEFs were cultured overnight on low or high stiffness hydrogels with FBS. A point-by-point height and stiffness maps of single cells was acquired from AFM-force volume mode measurements. Height images were overlaid with stiffness maps to determine localized mechanical properties for single cells. N=4 independent biological replicates. (B–C) MEFs infected with adenoviruses encoding LacZ or Rac<sup>V12</sup> plated on high stiffness hydrogels with FBS for 20 hours. (B) Fluorescence images of cells were acquired using Zeiss LSM 510 META/NLO confocal microscope; scale bar= 20  $\mu$ m. White arrows showed

lamellipodin localization at the leading edge. (C) Total cell lysates were analyzed by immunoblotting. N=3 independent biological replicates. (D–E) Starved MEFs transfected with control (ctrl) siRNA or a pool of siRNAs to lamellipodin (Lpd) were plated on low or high stiffness hydrogels with FBS and analyzed by AFM (D) or immunoblotting (E). Error bars show mean  $\pm$  SD; N=4 (D) and N=3 (E) independent biological replicates.